# A comparison of two parameterization schemes for condensation, clouds and precipitation by use of the Norwegian Limited Area Model: A three month parallel run

by

Erik Berge[1], Lars Anders Breivik[1] and Jón Egill Kristjansson[2]

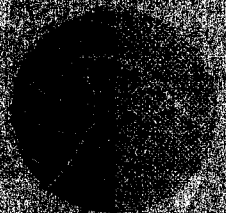

DNMI

Technical repoprt no. 133

Oslo October 1994

1. The Norwegian Meteorological Institute, Oslo, Norway
2. Department of Geophysics, University of Oslo, Norway

## Contents

## 1. Introduction

Modern weather services broadcast daily quite detailed forecasts of precipitation and clouds based on data from Numerical Weather Prediction (NWP) models. For the public these data are among the most important in a weather forecast. The precipitation forecasts are also of considerable use in areas such as agriculture, hydroelectric power and road traffic management (Bønsnes et al., 1993). At the same time, release of latent heat associated with the formation of clouds and precipitation has a pronounced impact on the development of low pressure systems, an effect that has been discussed in several studies (Sundqvist et al., 1989, Kristjánsson, 1990, Kuo and Reed, 1988, Breivik et al., 1992). Furthermore, several investigations have pointed out that clouds play an important role in many chemical processes in the atmosphere (Leliveld and Crutzen, 1991, Berge, 1993, Jonsson and Isaksen, 1993) by liquid phase chemical transformations and scavenging through precipitation. Thus, in order to evaluate the long range transport of air pollution accurately, reliable cloud and precipitation data over large areas are needed.

All the above mentioned areas involving clouds and precipitation processes must rely on information available from the NWP-models. For this reason, we feel there is a strong need for evaluation of existing parameterization schemes for condensation, clouds and precipitation. Hence, in this paper we present a comparison of the performance of two different schemes for condensation, clouds and precipitation. One of the schemes is used in the operational NWP-model of the Norwegian Meteorological Institute (DNMI), and it is described in Nordeng (1986, 1987). The other scheme is described in Sundqvist (1988) and has been used to investigate the links between low pressure development and clouds and precipitation for selected cases. Recently this scheme has been applied to a successful two week parallel run by the HIRLAM (High Resolution Limited Area Modelling) group (Gustafsson, 1993).

In the present study we have set up two parallel runs with a version of the NWP-model at DNMI having 50 km horizontal resolution. In the two runs only the schemes for condensation, clouds and precipitation differ. The parallel runs were made from October 1992 through December 1992. We compare forecasts of the parameters surface pressure, cloudiness and precipitation in order to evaluate the reliabilty of the schemes in connection with the applications mentioned in the previous section. Based on this evaluation, we hope to be able to make recommendations for improvements of the schemes and to suggest areas where further investigations are needed.

## 2. Parameterization of cloudiness and precipitation

In this section we present the basic (nor-50) and the Sundqvist (sund-50) parameterizations of condensation, cloud formation and precipitation. In particular we will emphasize their differences in order to better understand the results of the parallel runs.

### 2.1 Basic formulation

In a volume where condensation takes place, the basic variables in both condensation schemes are temperature (T), specific humidity (q) and cloud water (m). We may describe these three quantities by the prognostic equations

$$\frac{\partial T}{\partial t} = A(T) + \frac{L}{C_P}(Q - E_C - E_P) \tag{1}$$

$$\frac{\partial q}{\partial t} = A(q) - (Q - E_C - E_P) \tag{2}$$

$$\frac{\partial m}{\partial t} = A(m) + (Q - E_C - P) \tag{3}$$

The A( ) terms represent all other processes than condensation, evaporation and precipitation. A(T) and A(q) are treated exactly the same way in both models. The prognostic equation (3) is only fully solved in sund-50, while nor-50 neglects advection of cloud water, A(m). Furthermore, Q is the rate of condensation, P is the rate of conversion of cloud water to precipitation water, and $E_c$ and $E_p$ are the evaporation of cloud water and of precipitating water, respectively. Neither scheme includes a prognostic equation for P. In the following sections we will show how Q, P, $E_c$ and $E_p$ are parameterized. Also the formulas describing cloudiness, which is diagnostically derived in both schemes, will be given.

### 2.2 Stratiform condensation

The stratiform condensation is allowed to take place locally in a grid-box in both parameterizations. However, at mid-latitudes the stratiform cloud processes are in many cases related to large scale converging motions in frontal systems with extensive areas of clouds and precipitation. But, more isolated stratiform clouds such as stratocumulus and low stratus may also

occur outside the main frontal zones. Consequently, we expect the treatment of stratiform condensation to be of large importance for the average statistical results presented in this study.

### 2.2.1 The Nor-50

The parameterization of clouds and precipitation in nor-50 is documented in Nordeng (1986, 1987). The stratiform condensation follows the principle of the adjustment scheme described in Haltiner and Williams (1980). The condensation starts when a non-convective grid box becomes completely saturated and the excess humidity is converted to cloud water while the corresponding release of latent heat gives a temperature change. The temperature and humidity changes are found by solving the equations

$$q + \Delta q = q_s(T + \Delta T) \tag{4}$$

$$C_P \Delta T + L \Delta q = 0 \tag{5}$$

where $q_s$ is the specific humidity at saturation. Additionally, $\Delta m = -\Delta q$. Conversely, when cloudy air becomes subsaturated, cloud water is evaporated until saturation is reached by solving (4) and (5). The fractional cloudiness, b, in a grid-box is given by the diagnostic relation

$$b = \left( \frac{U - U_C}{1 - U_C} \right)^2 \tag{6}$$

where U denotes relative humidity, $U_c$ is the threshold relative humidity for clouds to exists. The threshold value equals 0.95 for clouds in the lowest model level, 0.85 in the next two layers and 0.75 further upward. At the three highest levels $U_c$ again increases to 0.95. In cases where U is less than $U_c$, b is simply equal to zero. Furthermore, in the lowest part of the troposphere the cloudiness is decreased in subsiding regions. The adjusted cloudiness, b', is given by

$$b' = b\left( \frac{\omega}{-10^3 hPa\left( s^{-1} \right)} \right) \tag{7}$$

where $\omega$ is the modelled vertical velocity (in hPa $s^{-1}$). In cases with positive omega (sinking motion) the cloudiness is put equal to zero. Obviously, (7) is bounded above by 1 and below by 0. Finally, the scheme does not allow surface clouds (fog) to develop if the potential temperature decreases with height.

### 2.2.2 The Sund-50

An important feature of the stratiform part of the Sundqvist scheme is that it allows for condensation to start before the whole grid-volume is saturated. Hence, the method requires a sub-grid treatment of clouds and condensation. Once the condensation has started the available humidity from large scale convergence and surface fluxes is partitioned between the cloud-free and cloudy parts of a grid-box (see Sundqvist, 1988, for a more detailed description). The release of latent heat, Q, averaged over a grid-box including sub-grid condensation is given by

$$Q = \frac{M - q_s \frac{\partial U}{\partial t}}{1 + \frac{U \varepsilon L^2 q_s}{R C_P T^2}} + E_C + E_P \tag{8}$$

where $q_s$ is the saturation specific humidity, L is latent heat of condensation, $c_p$ is the specific heat of dry air at constant pressure and R is the gas constant for dry air. Letting p denote pressure it can be shown that M, which is the convergence of available latent heat is given by

$$M = A(q) - \frac{U \varepsilon L q_s}{R T^2} A(T) + \frac{U q_s}{p} \frac{\partial p}{\partial t} \tag{9}$$

The terms on the right hand side of (9) represent condensation due to large scale convergence of humidity and temperature and local pressure changes respectively. Evaporation of cloud water is only allowed when cloud water is advected into a grid square where no condensation takes place.

The fractional cloudiness in a grid-box is calculated by the diagnostic relation

$$b = 1 - \sqrt{\frac{1 - U}{1 - U_{00}}} \tag{10}$$

Here $U_{00}$ is the threshold value for the onset of condensation which is set equal to 0.75 over land and 0.85 over sea. Approaching the surface from 850 hPa the onset relative humidity increases

linearly up to 0.975 for the lowest layer.

### 2.2.3 Comparison between nor-50 and sund-50

In Fig. 1 we show the dependence of cloud cover on grid-box averaged relative humidity in the stratiform case with a threshold value of 80%. We observe that the nor-50 gives less cloud coverage than sund-50 at relative humidities between 0.80 and 0.92, while near saturation nor-50 gives about 10% more cloud cover than does sund-50. In sum over the whole interval 0.8 - 1.0, the difference is close to zero.

An important difference between the two treatments of stratiform condensation concerns the criteria for the onset of condensation. Condensation processes will start earlier and probably exist over somewhat larger areas in sund-50. This may in turn influence the spatial distribution of the cloud- and precipitation systems. It is also clear from the formulae for fractional cloudiness that it will tend to increase more rapidly just after condensation has occurred in sund-50 than in nor-50.

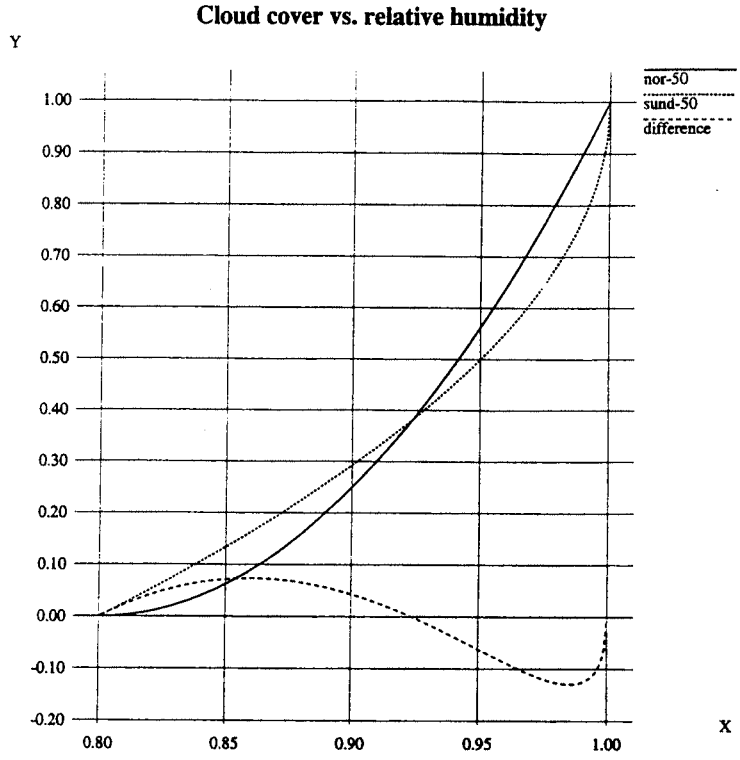


Figure 1: Cloud cover as a function of grid-box averaged relative humidity in a stratiform case assuming a threshold value of 80%. Solid line: nor-50; dottet line: sund-50; dashed line: difference (nor-50 - sund-50).

However, complete saturation in a grid-box may take place more rapidly in the nor-50 since no vapour is condensed before complete saturation of the grid-box. We would therefore also expect a more rapid evolution of full cloud coverage in a grid-box in nor-50 under conditions of increasing relative humidity (see (6)).

### 2.3 Convective condensation

Both the nor-50 and the sund-50 base the parameterization of convective condensation on the Kuo-scheme (Kuo 1965, 1974). Still there are some differences between the two formulations which will be elucidated in this section.

The driving mechanism for the development of convective clouds in the Kuo-scheme is the large scale convergence of moisture (including surface evaporation) in a convectively unstable atmosphere. The intensity of the convection is characterized by the so-called Kuo-parameter, $\xi$ which is defined as the available converging moisture in a column divided by the moisture necessary to saturate the whole column (i.e. fill the whole column with clouds). In order to initiate convective clouds in the Sundqvist scheme, surface air is lifted to its condensation level (LCL) and, if convectively unstable conditions are found above, convection starts. The nor-50 allows the convection to start at higher levels as well by searching for convectively unstable conditions through the whole column. In the sund-50 the convective heating rate is decreased with height implying relatively stronger heating near the surface. Such a distribution function is not applied to the nor-50.

In the sund-50 formulation, convective cloudiness is found by assuming a lifetime of the clouds, $\tau$, equal to 1 hour. The cloudiness, b, is then defined by

$$b = f\tau\xi \tag{11}$$

The factor f increases b when the cloud depth increases and/or the relative humidity increases, and it prevents b from approaching unity when $\xi$ is large (see Sundqvist et al., 1989). Recent studies of three cases with convective activity over the North Sea indicate that this formulation tends to underestimate the convective cloudiness although the spatial distribution is quite realistic (Kvamstø, 1993). In the nor-50 the fractional cloud coverage is determined as the largest of b' (see (7)) and $\tau\xi$, where $\tau$ is 15 mins. In comparison with the sund-50 scheme, this formulation will yield larger cloud fraction when the relative humidity is large, such that (7) is used. In showery situations in western Norway, this may in many cases be justified. But, according to Xu and Krueger (1991)

one should not generally expect relative humidity to be a good indicator of convective cloud cover. We also note that in the nor-50 formulation there is no restriction on the fractional cloudiness from approaching unity for increasing $\xi$. Hence, larger fractional cloudiness may be expected with the nor-50 than with sund-50 in convective situations.

Finally it should be noted that sund-50 precludes any stratiform condensation in a convective grid column, while nor-50 has no such restriction. This will again tend to favour larger cloud coverage from nor-50 than sund-50.

### 2.4 Release of precipitation

The local rate of release of precipitation in the sund-50 scheme is parameterized by the following formula

$$P = C_0 m \left[ 1 - e^{-\left(\frac{m}{bm_r}\right)^2} \right] \tag{12}$$

The parameter $c_0^{-1}$ gives a characteristic time for conversion of cloud droplets into precipitating drops, while $m_r$ is a threshold value for cloud water which m/b must exceed before the release of precipitation can become efficient. The values of $c_0$ are $10^{-3}s^{-1}$ and $10^{-4}s^{-1}$ in the convective and stratiform regime respectively, while $m_r$ equals $5 \cdot 10^{-4}$ for convection and $3 \cdot 10^{-4}$ for stratiform condensation. In order to crudely simulate the collision/coalescence process $c_0$ and $m_r$ are increased and decreased respectively depending on the amount of precipitation falling through the layer from above. Similarly, the effect of the ice phase is included, again by increasing $c_0$ and decreasing $m_r$ when the local temperature is lower than -5°C. A special treatment for precipitation release in cirrus clouds is also included (see Sundqvist, 1988). Evaporation of precipitation is only considered for stratiform precipitation, and the local rate of evaporation is a function of relative humidity, fractional cloudiness and the precipitation rate.

In nor-50 the local release of precipitation is given by the condensed water in excess of a critical cloud water mixing ratio of $5 \cdot 10^{-4}$ for temperatures above -12°C. For lower temperatures all condensed water is released as precipitation. Evaporation of precipitation in the nor-50 is calculated in nearly the same way as in sund-50.

We observe from the above that sund-50 allows for more water to be stored in the clouds, which obviously can affect the total release of precipitation. For example, in cases where the Bergeron-Findeisen mechanism is important, an earlier release of precipitation in nor-50 (due to

the release of all condensed matter as precipitation at temperatures below -12°C) may cause higher precipitation rates. On the other hand, a relatively small amount of water (typically 1 mm in a column) is stored in the clouds as compared to the accumulated precipitation at the ground, which in many cases mostly depends on the large scale convergence of vapour.

## 3. The test configuration

The two schemes, nor-50 and sund-50, have been compared within the framework of the operational limited area model at DNMI (Grønås and Hellevik, 1982, Nordeng, 1986). The version of the DNMI operational forecast model LAM50S used in this study covers 121 x 97 points on a polar stereographic map with 50 km horizontal resolution at 60°N. The number of vertical levels is 18, and in the vertical the sigma-coordinate is employed. The model area is shown on Fig. 2. The runs are made in a six hour intermittent data analysis/assimilation/forecast cycle.

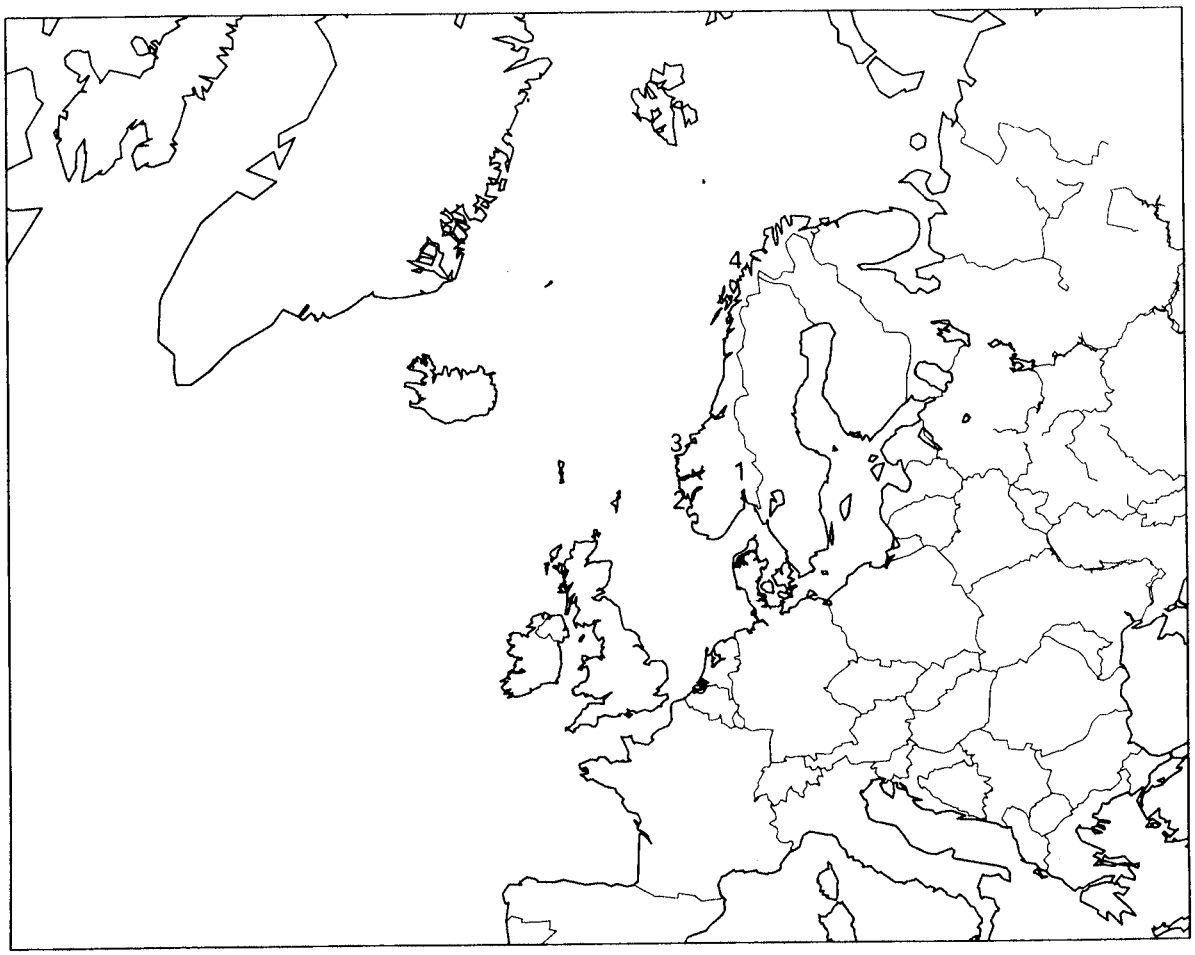


Figure 2: The LAM50S integration area and the position of the stations Evenstad (1), Bergen (2), Vigra (3) and Tromsø (4) .

In the analysis, observations from a time interval around the analysis time are used to correct a 6 hour forecast. The analysis method, which is a modification of the traditional successive correction method, was proposed by Bratseth (1986) and implemented for operational use at DNMI by
Grønås and Midtbø (1987). The three dimensional, multivariate analysis of wind, geopotential height and humidity is performed on 11 pressure levels.

In order to evaluate the impact of the two model versions, comparisons with conventional observations have been performed. The results from sund-50 and nor-50 were interpolated to synoptic stations and compared with observations. The synoptic stations were between 50 and 70 Norwegian inland and coastal stations. The collocation was employed for the three periods, 12 - 31 October, 2 - 30 November and 1 - 20 December, 1992. The statistical parameters used here and in the following are: bias, defined as the mean difference between model result and observation; STDE, standard deviation of the error, i.e. standard deviation of the differences between model results and the observations; RMSE, root mean square of the differences; CORR, correlation between model and observation results.

## 4. Results and discussions

In this section we present an evaluation of the results from the analysis/forecast cycles with sund-50 and nor-50, from October, November and December 1992, separately. The comparison with observations is focused on three parameters; surface pressure (MSLP), cloudiness and precipitation.

### 4.1 Surface pressure

Starting off with a typical example, time series of MSLP from Bergen (60°N, 5°E) in December 1992, are shown in Fig. 3. Solid, broken and dotted lines represent observations, and nor-50 and sund-50 predictions after a 36 hour forecast, respectively. Statistical parameters for the two model runs and a comparison between observations and each of the two model runs are given in the table below the time series. In the time series from Bergen shown on Fig. 3 the results are very similar for the two model versions, although sund-50 in this case yields slightly better results. Bias, STDE and RMSE are slightly lower in sund-50 than in nor-50.

The statistical results for model predictions of MSLP including all the observing stations are given in Table 1 and in Fig. 4. The results are shown for the three periods October, 92.10, November, 92.11, and December, 92.12. In all periods there were negative biases for both nor-50 and sund-50. In October nor-50 was slightly better with a RMSE of 3.64 mb as compared to 3.72

mb for sund-50. In November and December sund-50 gave better results and the differences were more significant. The RMSE for nor-50 was 5.50 mb and 5.17 mb while the corresponding values for sund-50 were 4.27 mb and 4.97 mb. A scatter plot of the RMSE comparing the two models including all three periods is presented in Fig. 5. The crosses are for October, X's for November and Y's for December. Marks along the dotted line indicate equal performance of the two model versions. The figure visualizes the result of Table 1 that the RMSE was on average somewhat lower for sund-50 than for nor-50.

This result is consistent with findings of a HIRLAM study (Gustafsson, 1993) where the operational HIRLAM model was compared to a parallel run using the Sundqvist scheme. Their runs were for two weeks in October 1992 and a comparison with about 40 synoptic stations showed reduced RMSE compared to the operational model. Several case studies also confirm that intense lows are better simulated with the sund-50 than in nor-50 (Sundqvist et al., 1989, Kristjánsson, 1990, Breivik et al., 1992). Breivik et al. (1992) pointed out that the nor-50 has a tendency to underestimate the later stages of storm development, and that the introduction of the sund-50 condensation scheme gives better results in these cases. The early phase of an explosive cyclone development in mid-latitudes is typically characterized by baroclinic energy conversions, while in the later stages the release of latent heat often plays a more important role. As suggested by Shapiro and Keyser (1990) this probably has to do with the production of potential vorticity (PV) at low levels through latent heat release in the back-bent frontal zone.

Having found an improvement by sund-50 on synoptic scale forecasts of MSLP, one would expect to find some improvement of the forecasts of cloud cover and precipitation as well.

### 4.2 Cloud cover

The cloud parameter employed was the midday observed cloud cover, i.e., the two-dimensional coverage of the sky in octas as observed from the ground by an observer. These measurements were compared to the two-dimensional cloud cover taken from the models by assuming random/maximum overlapping of the clouds in a vertical column after a 36 hour forecast. It is important to bear in mind the difficulties in observing cloud cover correctly, especially due to horizontal overlapping of clouds and the reduced sky view at stations surrounded by mountains. But, the synoptic surface measurements were the only long term data series available to evaluate the cloudiness.

As before we will start by looking at a couple of typical examples from the synoptic stations. Fig. 6 upper panel shows a time series from Bergen in December 1992. The solid line represents the observation, the broken line nor-50 and the dotted line sund-50. For this station the

statistical performance as measured in bias, STDE and RMSE gave better results for nor-50 than for sund-50. Fig. 6 lower panel shows a similar series for Tromsø (70°N, 19°E). Here the negative bias is larger for sund-50, while STDE is smaller, 27 % compared to 31 %. It should be noted that the values above 100 % are due to the coding of fog which is given as nine octas (112.5 %).

We also observe from the time series that nor-50 very often yields nearly 100% coverage while somewhat lower values are seen in many cases in both the observations and in sund-50. The reason for this is probably that nor-50 has no sub-grid treatment of the condensation. It allows a grid-box to become absolutely saturated before any condensation starts (eqs. (4)-(5)). This implies that complete saturation in a grid-box is achieved relatively quickly. Furthermore, this implies 100% cloud cover according to (6). In sund-50 the sub-grid condensation will consume some of the humidity; consequently a 100% cloud coverage is not obtained as easily as in nor-50. Furthermore, in Table 2 and Fig. 7 we present (similar to Table 1 and Fig. 4 for surface pressure) the statistics from the three periods for cloud cover using all stations. It is seen that sund-50 correlates better with the observations. Again this is probably due to the sub-grid scale treatment which gives a more realistic description of the variation of the partial cloudiness. If we look further at the averaged results as presented in Table 2 and Fig. 7 we see that for October, November and December the biases in cloud cover were respectively - 9.55%, - 13.42% and - 14.20% for sund-50 while the corresponding numbers were - 5.75%, - 4.85% and 0.32% for nor-50. Fig. 8 a,b and c show scatter plots comparing the bias in cloud cover of sund-50 and nor-50 from the three months. The figures illustrate the negative bias in sund-50 in all three periods while there is a more random distribution of errors in nor-50. The scatter is large for both models.

Another interesting feature of the cloud fields was seen in the vertical profiles. For all cases examined we found less high level cloudiness in sund-50 than in nor-50. On the other hand we saw larger areas with low level clouds in sund-50; still the fractional cloudiness in nor-50 seems to be larger in frontal zones. An example of this is given in Figs. 9a and b for low clouds and in Figs. 9c and d for high cloud. The figures shows the cloud cover in the model integration area 00 UTC 12 December 1992. The heavy shaded areas indicate total cover while partly shaded, dotted areas indicate partly clouded areas. Fig. 9a and b shows a larger area of partly low level cloud cover in sund-50. On the other hand Figs. 9c and d show larger areas of high level clouds in nor-50 compared to sund-50 in this situation.

In order to analyze geographical dependencies in the results the average differences between forecasts and observations were plotted in a horizontal regular grid. The differences were interpolated from the irregular observation grid to a regular grid by use of simple kriging. In Figs. 10a,b,c and d we present the kriged difference fields for cloudiness in November and December

1992 for the two models. We see that the spatial variance is well correlated in the two models, but in nearly all areas the sund-50 yields larger underestimation. The underestimation is particularly pronounced in the northwestern part of southern Norway. Also in December the kriged patterns follow each other quite closely, but the nor-50 gives systematically higher values in all areas including those with overestimated cloudiness.

Holding this together with the vertical variation of the cloudiness it could be suggested that the large negative bias in sund-50 is coupled either to an underestimation of (thin) cirrus clouds and/or low convective clouds. A closer look at the data shows that in November 1992 southeasterly winds with many frontal passages dominated the weather pattern in southern Norway. This in turn gave rise to quite large amounts of precipitation and dense cloud coverage in southeastern Norway. In contrast, December was dominated by southwesterly winds and the largest precipitation amounts fell in western and northwestern parts of southern Norway. In this situation high (cirrus) clouds were more frequently observed on the north-western (lee) side of the mountains in November compared to December. In eastern Norway the opposite was the case with more "lee-type" meteorology in December. This is illustrated by a look at the frequency of high and low clouds at the synoptic station Vigra (62.6°N, 6.1°E) in northwest Norway and at Evenstad (61.4°N, 11.1°E) in southeastern Norway as shown in Table 3. The table shows that the frequency of high clouds at Vigra was about twice as large in November as in December. If we look at the occurrence of convective clouds we see that it is somewhat larger in December than in November. As already mentioned the underestimation of the cloudiness could be related to the description of the convective cloud cover in sund-50, in particular in December. In November the total observed cloudiness in northwestern Norway is more influenced by high clouds which may have contributed to the underestimation. In fact we see the same tendency although not very strongly, in eastern Norway at Evenstad where a larger underestimation of the cloudiness in December coincides with more typical "lee-type" meteorology and slightly higher frequency of high clouds together with a lower frequency of low clouds compared to the November data.

In order to understand these differences we first consider the treatment of cirrus clouds in the two schemes. It is important to notice that in nor-50 there is no direct coupling between the cirrus clouds and precipitation. The cirrus clouds form at 95% relative humidity where they immediately nearly fill one grid-box. This explains why there were more high clouds present in the nor-50 runs as discussed above. In nor-50 very often either complete cloudiness or cloudfree conditions were seen. The precipitation release does however not start before 100% relative humidity. This gives the clouds (or the relative humidity) some time to build up before precipitation release begins. In sund-50, however, a very effective release of ice crystals will start

in the fractional cirrus clouds, and hence they can not grow as easily as in nor-50. Based on the above results, it is possible that the sund-50 should allow for some more cirrus clouds to develop than what is the case today. Another possible explanation is that in the code for sund-50 applied here no stratiform clouds were permitted above convective clouds. Hence if a grid column was defined as convective, with perhaps quite shallow convection the highest levels would remain cloudfree regardless of the relative humidity.

The convection that prevails at the western coast of Norway in wintertime is often deep and in many cases it gives rise to nearly full cloud coverage. At the coastal station Vigra more than 60% of the days with convection in November and December 1992 had either 7 or 8 octas of cloud coverage. As explained in subsection 2.3 we would expect nor-50 to give larger cloud cover in such situations, due to its larger dependency on relative humidity.

Summarizing the above results it is clearly indicated that both models have problems with the cloud formulation. Nor-50 seems to predict better the total cloud cover measured in mean differences between forecast and observation. However the lower values of STDE for sund-50, consistent with the higher correlation, indicates that the physical processes causing the variations in cloud cover might be better formulated in sund-50. If so, an improvement of the results depends on the possibility to find and remove the cause of the bias, and maybe there is a larger potential for improvements in the sund-50 than in nor-50 with the present diagnostic formulae for cloud cover. It is also important to keep in mind that the cloud cover may be somewhat overestimated by the observers at the synoptic stations as already pointed out earlier in this section.

### 4.3 Precipitation

To evaluate the results for precipitation we have used observations of 12 hour accumulated precipitation measured daily at 18 UTC. The measurements were compared to model accumulated 12 hour precipitation between 30 and 42 hour prognostic time, starting from 00 UTC. A time series similar to Figs. 3 and 6 is shown in Fig. 11. The station is Bergen and the period was again December 1992. The curves for sund-50 and nor-50 follow each other qualitatively but the amounts of precipitation are different. There was less precipitation in sund-50 than nor-50 for this station and period, and both model versions underestimate the precipitation summed over the whole month.

This tendency seems to hold when the results are averaged over all the observing stations from the three periods, as shown in Table 4 and Fig. 12. To produce the statistics presented in this table, only the cases where the observed precipitation exceeded 0.5 mm were used. It is seen from the table that there was an underestimation in both models, although the negative bias was largest

in sund-50 in all three periods. In October the results measured in STDE, RMSE and correlation were significantly better for nor-50 than for sund-50. In November the correlations for both models were very low. In December as well as November sund-50 was slightly better than nor-50 measured in STDE. The overall impression is that sund-50 underestimates the precipitation somewhat more than the nor-50. This tendency also holds when we include the cases with less than 0.5 mm in the statistics. In December nor-50 slightly overestimates precipitation. It is interesting to note that this is consistent with an overestimation of the cloudiness for the same month.

In Figs. 13a,b,c and d we also present the geographical distribution of the kriged differences in precipitation for November and December 1992. It is seen that somewhat less precipitation is produced in sund-50 than in nor-50 in nearly all areas including both those with over- and underestimations. However, the patterns of the two models follow each other quite closely, indicating that the areas of over- and underestimation are largely determined by the model dynamics. This is what we would expect since the main mechanism for formation of precipitation is the large scale convergence of humidity, which is quite independent of the cloud parameterization schemes. The only source for differences in this term is the feedback from the treatment of the condensation processes on the large scale dynamics of the model.

Based on the above results it is somewhat surprising that the precipitation in sund-50 is so much lower than in nor-50 in many cases although it is possible that the differences in pressure distribution could explain this. As already mentioned in Section 2.4 differences may also arise since more liquid water is stored in the clouds in sund-50. However, Tables 2 and 4 show that a negative bias in precipitation is correlated with a negative bias in cloudiness. Case studies with the Sundqvist scheme (Raustein et al., 1991, Kvamstø, 1991) indicate realistic vertically integrated cloud water amounts. Another possibility is the mechanism for precipitation release. It is possible that the more effective release of precipitation in nor-50 (all condensate falls out immediately when the temperature is below -12°C) helps to initiate and give higher precipitation rates through the seeder-feeder mechanism that occurs when precipitation from above falls through lower clouds. However, we do not feel that a fully satisfactory and complete explanation can be given to this problem based on the present analysis. It would probably be desirable to include a complete hydrological budget for the two models in order to be able to better understand the observed differences in precipitation amounts.

## 5. Conclusions and recommendations.

In this paper the "Sundqvist scheme" (sund-50) for clouds and condensation has been compared with the operational version (nor-50) of the cloud parameterization within the limited

area model at the Norwegian Meteorological Institute. We have set up two parallel runs with a version of the NWP-model at DNMI where only the two schemes for condensation, clouds and precipitation differ. The parallel runs were made for nearly three months from October 1992 through December 1992, and the model results for surface pressure, precipitation and two-dimensional cloudiness were verified daily by use of about 50 Norwegian synoptic stations.

In our evaluation the sund-50 yields the best scores for surface pressure for two months, while in October nor-50 and sund-50 give very similar results. Averaged over one month the bias varies from -2.32 hPa to -1.12 hPa while the correlation ranges from 0.91 to 0.96. These results are consistent with earlier case studies, and they are probably due to a more realistic description of the release of latent heat in conjunction with mid-latitude synoptic disturbances in the sund-50 compared to the nor-50.

For the two-dimensional cloudiness a quite large negative bias from -9.55 % in October to -14.20% in December is observed in sund-50. A somewhat smaller underestimation is seen in nor-50 for October and November, while a small overestimation is found in December. However, the sund-50 has somewhat better correlation with the data than the nor-50. We also observe that the nor-50 has a larger tendency to give either full cloud coverage or clear skies. Our interpretation of this is that the sund-50 gives a more physical description of the cloudiness than the nor-50. The large negative bias in sund-50 could be related to an underestimation of high (cirrus) clouds and convective cloudiness, in particular during deep convection. Improvements of the sund-50 may be sought in these areas. Improvements of the nor-50 would probably require a sub-grid treatment as already applied in the sund-50.

The precipitation fields are underestimated in both models (except for the nor-50 in December), and the largest negative bias of -2.29 mm is found for November in the sund-50. The overall impression is that the sund-50 yields larger underestimation than the nor-50. In terms of standard deviation however, the sund-50 is slightly better for two months. The release of precipitation is somewhat more efficient in the nor-50 for clouds with temperatures below -12°C which could account for some of these differences. But since the precipitation is largely determined by the large scale convergence of humidity and not the water storage in clouds it is likely that the differences in precipitation can be caused by some other reasons as well. A full analysis of the hydrological budgets of the two models could possibly reveal this better in the future.

## 6. Acknowledgments

We would like to express our appreciation for the assistance by Mr. A. Foss in setting up

the Sund-50 model version in an operational mode on a CRAY Y-MP4D/464 at the Technical University of Norway in Trondheim.

## 7. References


Bratseth, A.M., 1986. Statistical interpolation by means of successive corrections, Tellus, 38A, 439 - 447.

Breivik, L. A., Kristjánsson, J. E., Midtbø, K. H., Røsting, B., and Sunde, J., 1992. Simulations of the 1 January 1992 North Atlantic storm. DNMI Techn. Rep. No. 99.

Bønsnes, T, Hjøllo, B. A. and Odegaard, V., 1993. Prognoser for Kraftverksformaal. Erfaring med oekt opploesning i atmosfaeremodeller, Statistisk korreksjon av nedboerprognoser. MIPS Report nr. 2/93, in Norwegian.

Grønås, S., and O.E. Hellevik, 1982. A limited area prediction model at the Norwegian Meteorological Institute. DNMI Techn. Rep. No. 61.

Grønås, S., and K.H. Midtbø, 1987. Operational multivariate analysis by successive corrections. J. Meteorol. Soc. Jpn., WMO/IUGG/NWP Symp., Spec. issue, 61-74.

Gustafsson, N., (ed.) 1993. Hirlam 2 final report. Hirlam Technical Report No. 9, 126 pp.

Kristjánsson, J. E., 1990. Model simulations of an intense meso-β scale cyclone: The role of condensation parameterization. Tellus 42A, 78-91.

Kuo, H. L., 1965. On formation and intensification of tropical cyclones through latent heat release by cumulus convection. J. Atmos. Sci., 22, 40-63.

Kuo, H. L., 1974. Further studies of the parameterization of the influence of cumulus convection on large-scale flow. J. Atmos. Sci., 31, 1232-1240.

Kuo, Y.-H. and R. J. Reed, 1988. Numerical simulations of an explosively deepening cyclone in the eastern Pacific. Mon. Wea. Rev., 116, 2081-2105.

Kvamstø, N. G., 1991. An investigation of diagnostic relations between stratiform fractional cloud cover and other meteorological parameters in numerical weather prediction models. J. Appl. Met., 30, 200-216.

Kvamstø, N. G., 1993. An investigation of the cumulus cloudiness parameterization in northerly flows in the Norwegian Sea. Mon. Wea. Rev., 121, 1434-1449.

Nordeng, T.E., 1986. Parameterization of physical processes in a three dimensional numerical weather prediction model. DNMI Techn. Rep. No. 65.

Nordeng, T.E., 1987. The effect of vertical and slantwise convection on the simulation of polar lows. Tellus 39A, 354-375.

Raustein, E., Sundqvist, H., and Katsaros, K., 1991. Quantitative comparison between simulated cloudiness and clouds objectively derived from satellite data. Tellus, 43A, 306-320.

Shapiro, M.A., and Keyser, D., 1990. Fronts, jet streams and the tropopause. In: Extratropical Cyclones, C. Newton and E. Holopainen (ed.), American Meteorological Society, Boston, 167-191.

Sundqvist, H., 1988. Parameterization of condensation and clouds in models for weather prediction and general circulation simulation. In Physically-based modelling and simulation of climate and climatic change, M.E. Schlesinger (ed.), Reidel, Dordrecht, 433-461.

Sundqvist, H., Berge, E., and Kristjánsson, J. E., 1989. Condensation and cloud parameterization studies with a mesoscale numerical weather prediction model. Mon. Wea. Rev., 117, 1641-1657.

Xu, K.-M., and Krueger, S. K., 1991. Evaluation of cloudiness parameterizations using a cumulus ensemble model. Mon. Wea. Rev. 119, 342-367.

## Appendix A. Tables 1-4.

| Model | Parameter | Period | Npos | N | Bias | STDE | RMSE | Corr |
|---|---|---|---|---|---|---|---|---|
| nor-50 | mslp | 92.10 | 56 | 1023 | -2.26 | 2.85 | 3.64 | 0.92 |
| sund-50 | mslp | 92.10 | 56 | 1023 | -2.32 | 2.91 | 3.72 | 0.92 |
| nor-50 | mslp | 92.11 | 57 | 1428 | -1.78 | 5.20 | 5.50 | 0.91 |
| sund-50 | mslp | 92.11 | 57 | 1428 | -1.12 | 4.12 | 4.27 | 0.94 |
| nor-50 | mslp | 92.12 | 59 | 1079 | -2.06 | 4.74 | 5.17 | 0.96 |
| sund-50 | mslp | 92.12 | 59 | 1079 | -1.76 | 4.65 | 4.97 | 0.96 |

Table 1: Model results from nor-50 and sund-50 forecasts of mean sea level pressure + 36 hours compared to synoptic observations. Npos is the number of observing stations used in the statistics, while N is the total numbers of entries. The statistics are shown for three periods, October (92.10), November (92.11) and December (92.12) 1992. Bias is differences between model results and observation, and STDE and RMSE is standard deviation and root mean square of the differences. 'Corr' is the correlation.

| Model | Parameter | Period | Npos | N | Bias | STDE | RMSE | Corr |
|---|---|---|---|---|---|---|---|---|
| nor-50 | total cl (%) | 92.10 | 66 | 1210 | -5.72 | 42.20 | 42.59 | 0.37 |
| sund-50 | total cl (%) | 92.10 | 66 | 1210 | -9.55 | 36.50 | 37.73 | 0.42 |
| nor-50 | total cl (%) | 92.11 | 67 | 1678 | -4.85 | 38.72 | 39.02 | 0.37 |
| sund-50 | total cl (%) | 92.11 | 67 | 1679 | -13.42 | 35.05 | 37.53 | 0.42 |
| nor-50 | total cl (%) | 92.12 | 69 | 1257 | 0.32 | 32.94 | 32.94 | 0.47 |
| sund-50 | total cl (%) | 92.12 | 69 | 1260 | -14.20 | 31.83 | 34.86 | 0.47 |

Table 2: Model results from nor-50 and sund-50 forecasts of total cloud amount + 36 hours compared to synoptic observations. Npos is the number of observing stations used in the statistics, while N is the total numbers of entries. The statistics are shown for three periods, October (92.10), November (92.11) and December (92.12) 1992. Bias is differences between model results and observation, and STDE and RMSE is standard deviation and root mean square of the differences. 'Corr' is the correlation.

**TABLE 3.** Frequency of 12 UTC observed cloudiness for the two norwegian synoptic stations Vigra and Evenstad (see Fig. 2 for location of the stations) during November and December 1992.

| **Vigra** | **November 1992 2-30** | **December 1992 1-20** |
|---|---|---|
| Low clouds | 25 (0.87) | 19 (0.95) |
| Low stratus clouds | 9 (0.36) | 5 (0.26) |
| Low convective clouds | 16 (0.64) | 14 (0.74) |
| Medium clouds | 22 (0.76) | 16 (0.8) |
| High clouds | 14 (0.48) | 5 (0.25) |

| **Evenstad** | **November 1992 2-30** | **December 1992 1-20** |
|---|---|---|
| Low clouds | 29(1.00) | 16 (0.80) |
| Low stratus clouds | 26 (0.90) | 14 (0.74) |
| Low convective clouds | 3 (0.10) | 2 (0.12) |
| Medium clouds | 24 (0.83) | 16 (0.80) |
| High clouds | 10 (0.34) | 8 (0.40) |

| **Model** | **Parameter** | **Period** | **Npos** | **N** | **Bias** | **STDE** | **RMSE** | **Corr** |
|---|---|---|---|---|---|---|---|---|
| nor-50 | precip. | 92.10 | 49 | 260 | -1.51 | 3.16 | 3.50 | 0.57 |
| sund-50 | precip. | 92.10 | 49 | 260 | -1.85 | 3.72 | 4.16 | 0.28 |
| nor-50 | precip. | 92.11 | 63 | 546 | -1.59 | 5.19 | 5.43 | 0.06 |
| sund-50 | precip. | 92.11 | 63 | 546 | -2.29 | 5.14 | 5.63 | 0.04 |
| nor-50 | precip. | 92.12 | 64 | 477 | 0.14 | 5.51 | 5.51 | 0.46 |
| sund-50 | precip. | 92.12 | 64 | 477 | - 1.34 | 5.12 | 5.30 | 0.38 |

Table 4: Model results from nor-50 and sund-50 forecasts of 12 hours accumulated precipitation +30 - +42 hours compared to synoptic observations. Npos is the number of observing stations used in the statistics, while N is the total numbers of entries. The statistics are shown for three periods, October (92.10), November (92.11) and December (92.12) 1992. Bias is differences between model results and observation, and STDE and RMSE is standard deviation and root mean square of the differences. 'Corr' is the correlation.

## Appendix B. Figures 3-13.

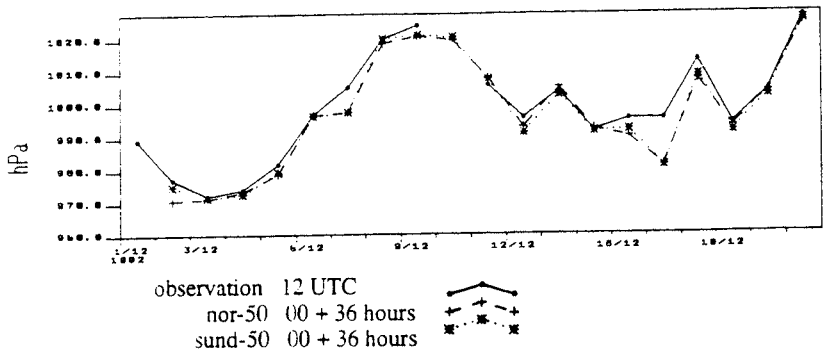


| | STDE | RMSE | BIAS | CORR | N |
|---|---|---|---|---|---|
| nor-50 | 3.8 | 4.8 | -2.8 | 0.97 | 18 |
| sund-50 | 3.5 | 4.5 | -2.7 | 0.98 | 18 |

Figure 3: Time series comparing 36 hour model forecasts with observed values of MSLP from Bergen in December 1992. Solid, broken and dotted lines represent observations, nor-50 and sund-50 respectively. Statistical parameters for sund-50 and nor-50 comparing with observation are given in the table.

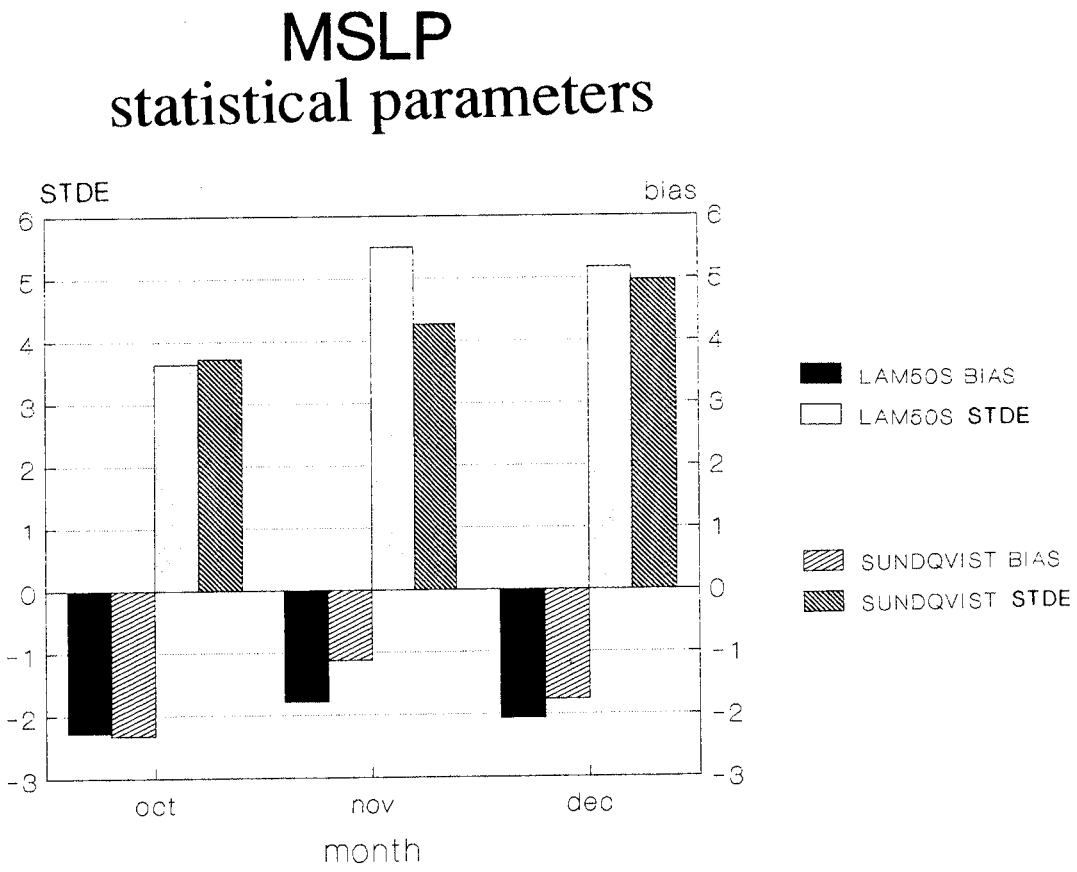


Figure 4: Standard deviation of errors, STDE, and bias for 36 hour model forecasts of MSLP. The results include all the observing stations and are given for the three periods October, November and December.

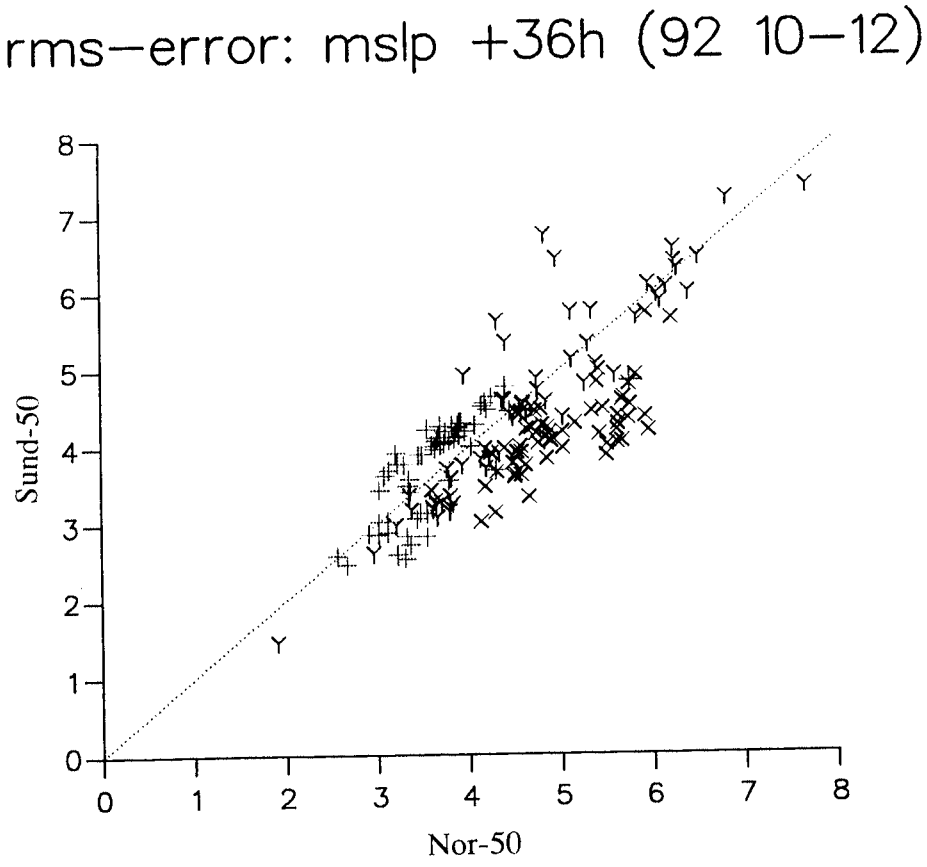


Figure 5: Scatter plot of root mean square error, RMSE, of 36 hour forecasts of MSLP comparing the two models. Horizontal axis gives the results for nor-50 and vertical for sund-50. The crosses are for October, X's for November and Y's for December. Marks along the dotted line indicate equal performance of the two models.

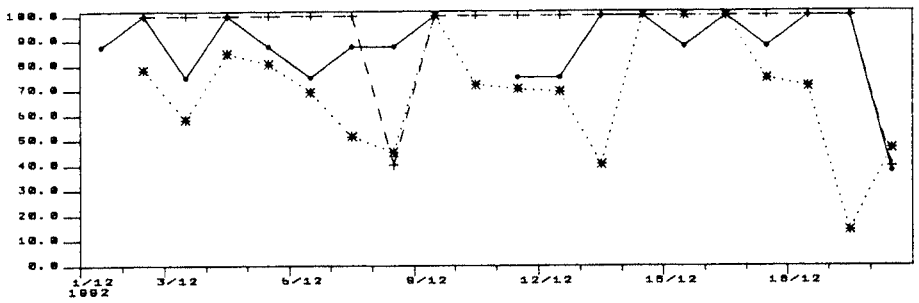

observation 12 UTC
nor-50 00 + 36 hours
sund-50 00 + 36 hours

| | STDE | RMSE | BIAS | CORR | N |
|---|---|---|---|---|---|
| nor-50 | 16.3 | 17.3 | 5.8 | 0.57 | 18 |
| sund-50 | 24.3 | 30.2 | -17.8 | 0.26 | 18 |

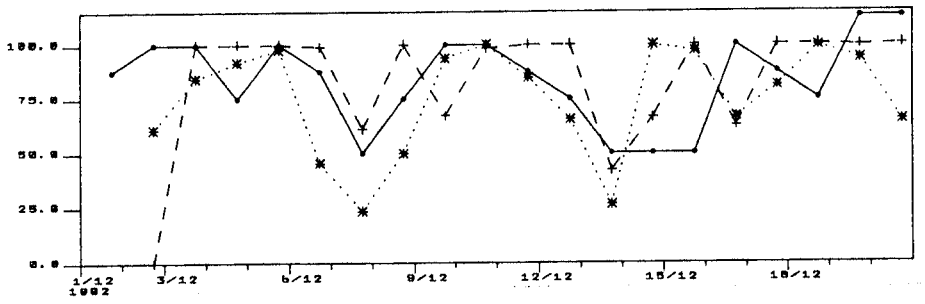

observation 12 UTC
nor-50 00 + 36 hours
sund-50 00 + 36 hours

| | STDE | RMSE | BIAS | CORR | N |
|---|---|---|---|---|---|
| nor-50 | 31.4 | 31.4 | 0.4 | 0.14 | 19 |
| sund-50 | 26.7 | 28.0 | -8.5 | 0.30 | 19 |

Figure 6: Similar time series as Figure 3, but for total cloud cover given in %. Upper panel shows a time series from Bergen in December 1992. The solid line represents the observation, the broken line nor-50 and the dotted line sund-50. Lower panel shows a similar series for Tromsø (70°N, 19°E). It should be noted that the values above 100 % are due to the coding of fog which is given as nine octas (112.5 %).

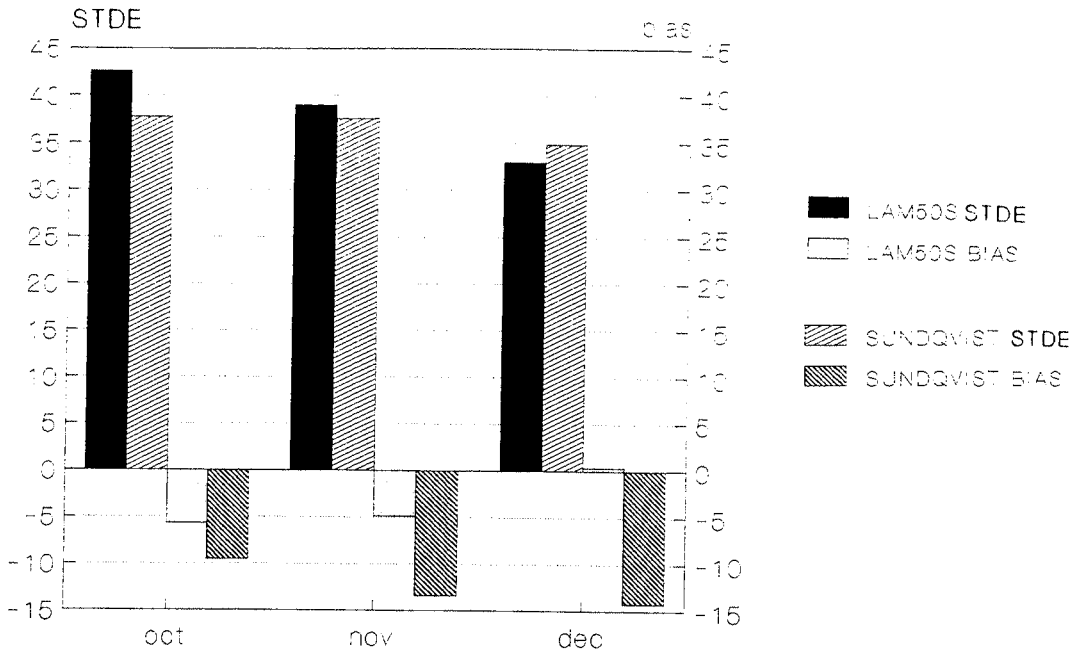


Figure 7: Standard deviation of errors, STDE, and bias for 36 hours model forecasts of total cloud cover. The results include all the observing stations and are given for the three periods October, November and December.

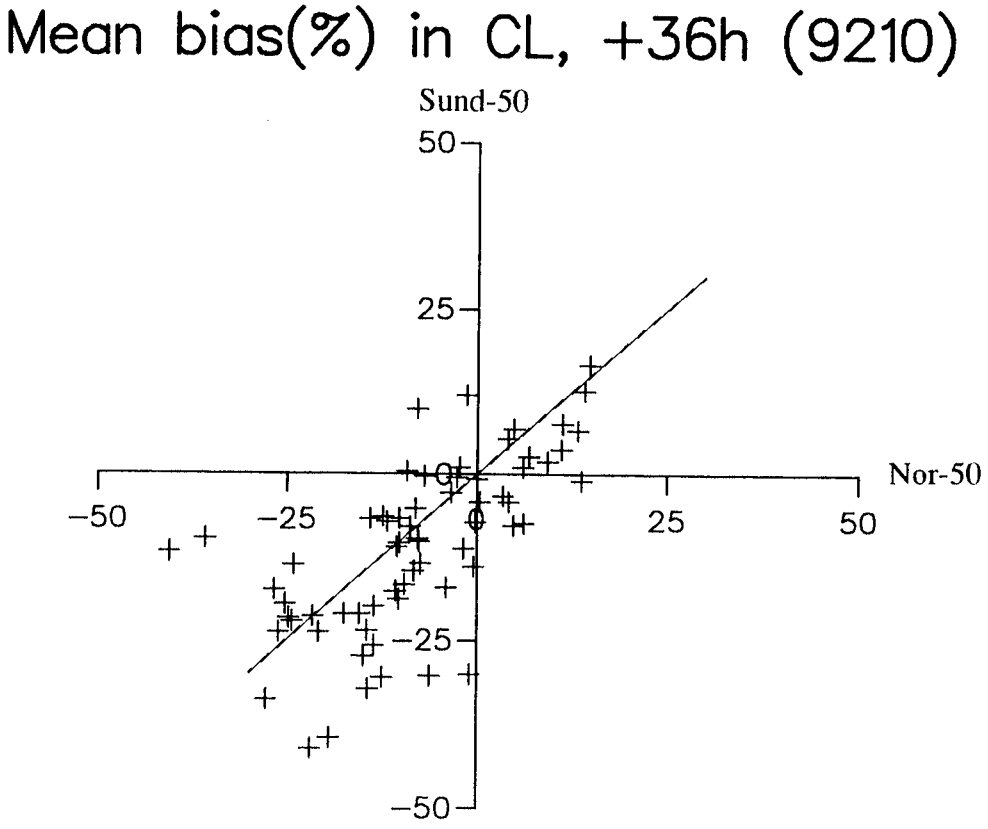


Figure 8a: Scatter plots comparing the bias in cloud cover of sund-50, vertical axis, and nor-50, horizontal axis, for October 1992.

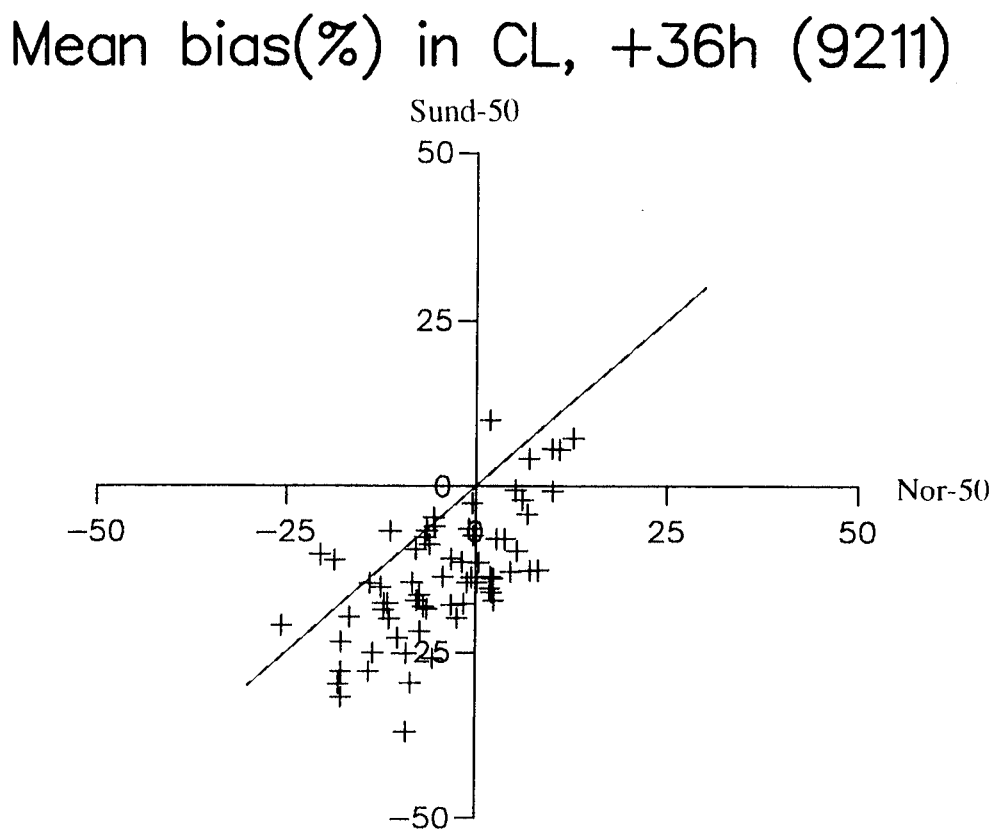


Figure 8b: As Fig. 8a, but for November 1992.

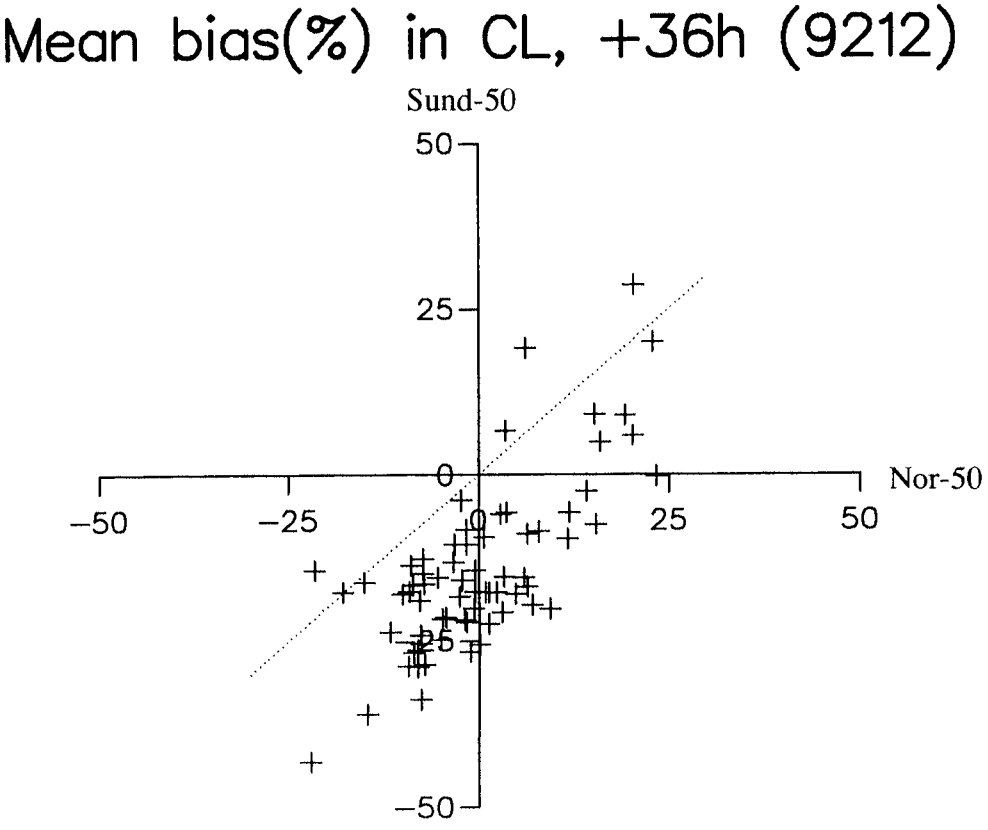


Figure 8c: As Fig. 8a, but for December 1992.

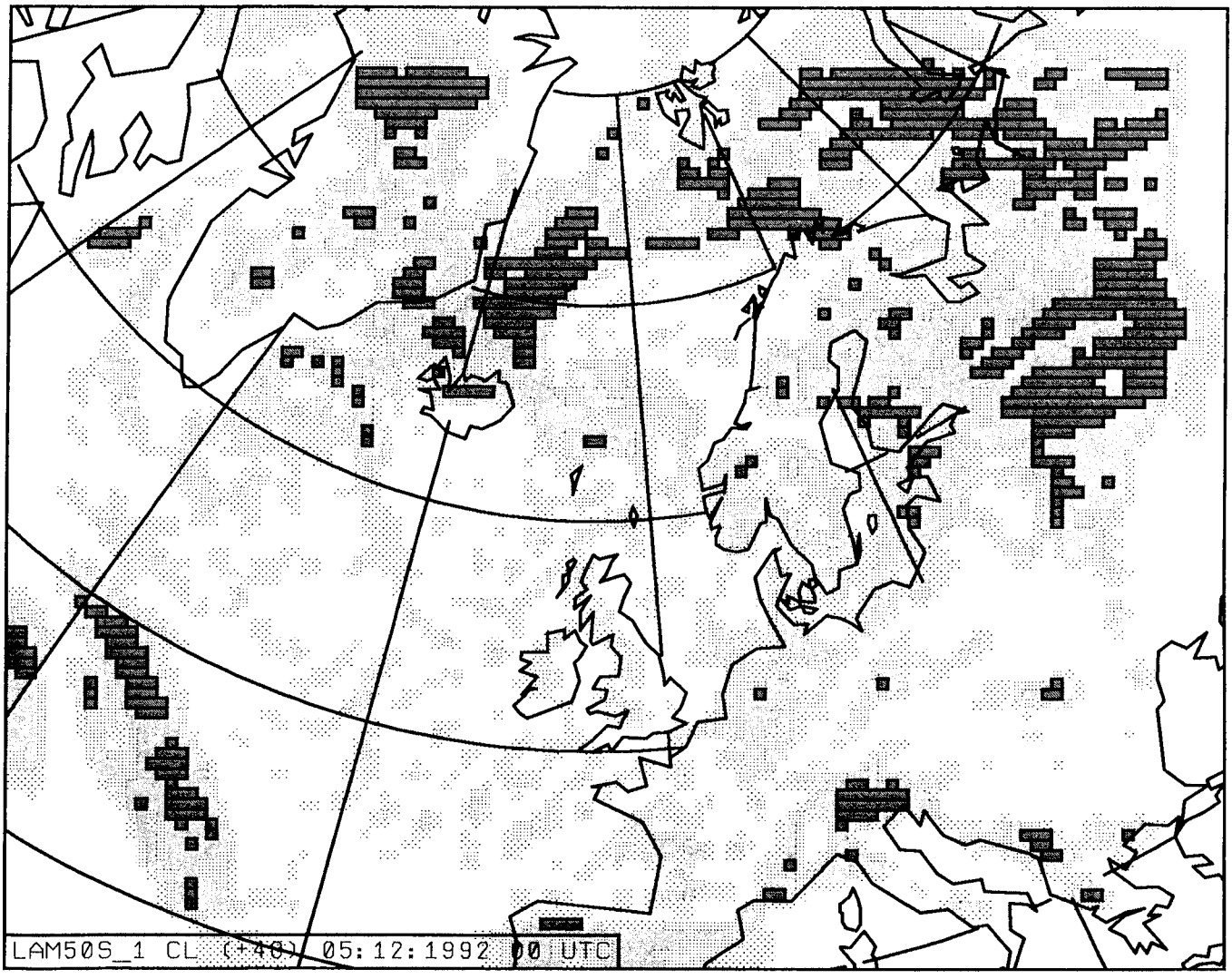


Figure 9a: Cloud cover for low clouds using sund-50 at 00 UTC, 5 December 1992. The heavy shaded areas indicate total cover while partly shaded, dotted areas indicate partly clouded areas.

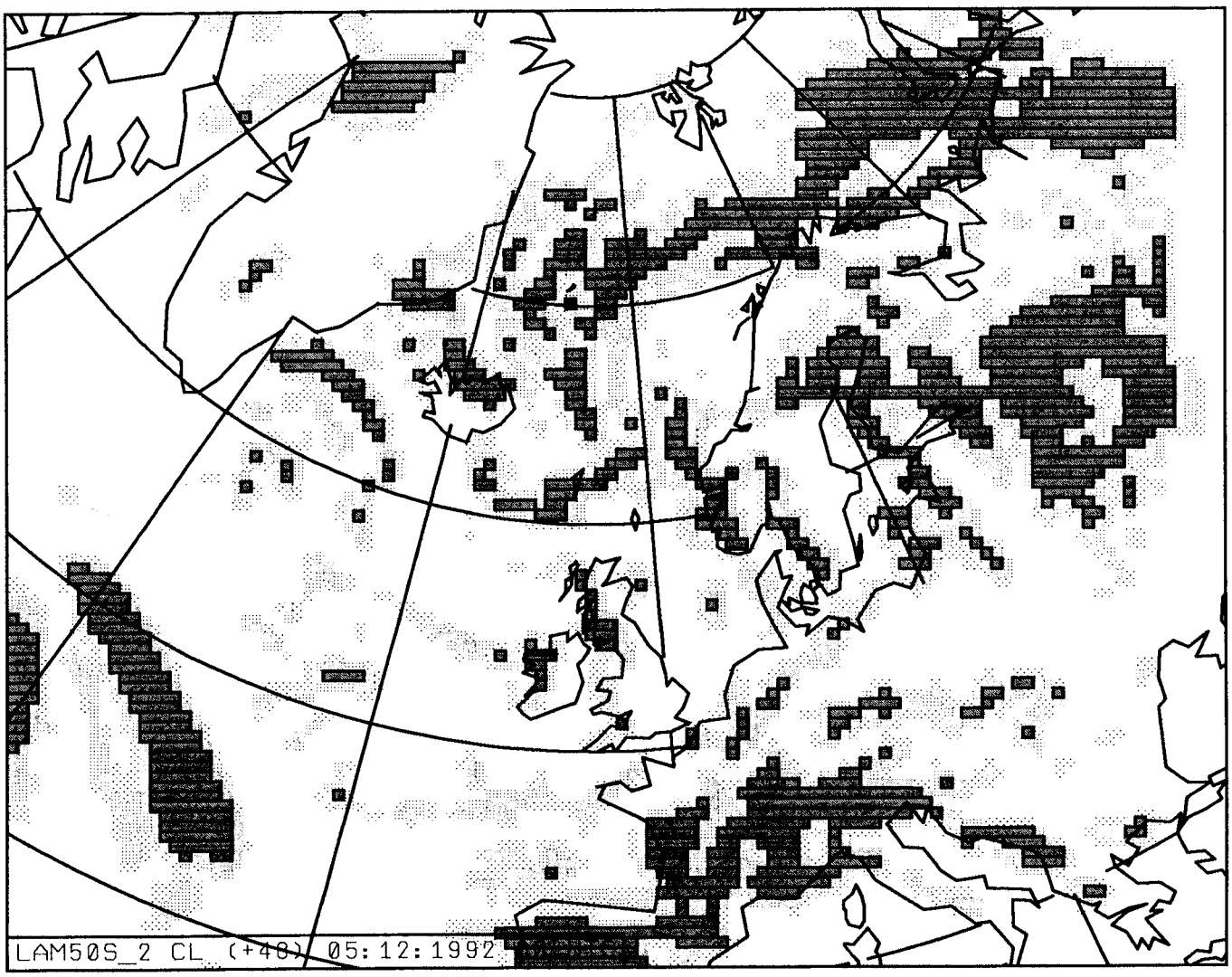


Figure 9b: As Fig. 9a, but for low clouds using nor-50.

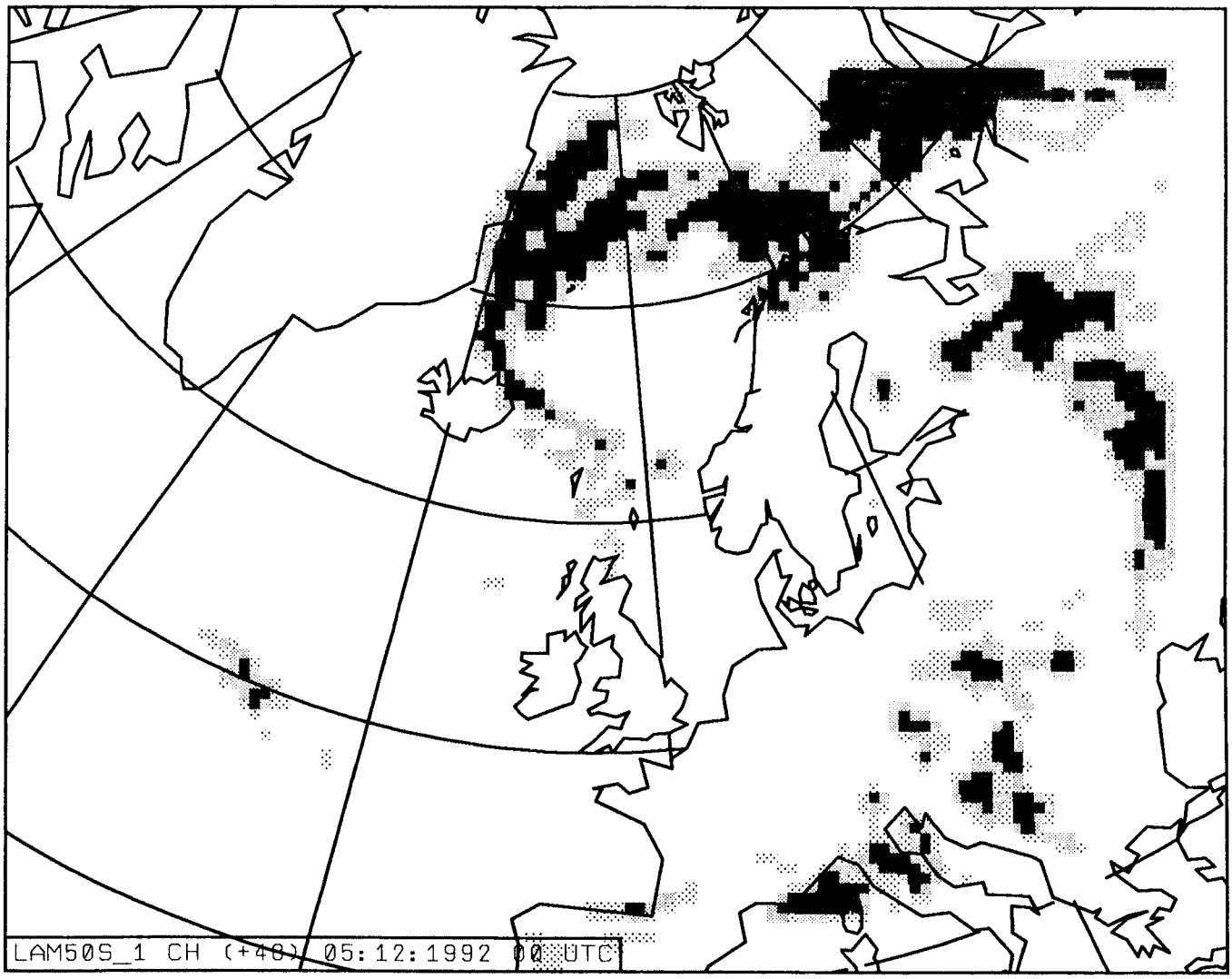


Figure 9c: As Fig. 9a, but for high clouds using sund-50.

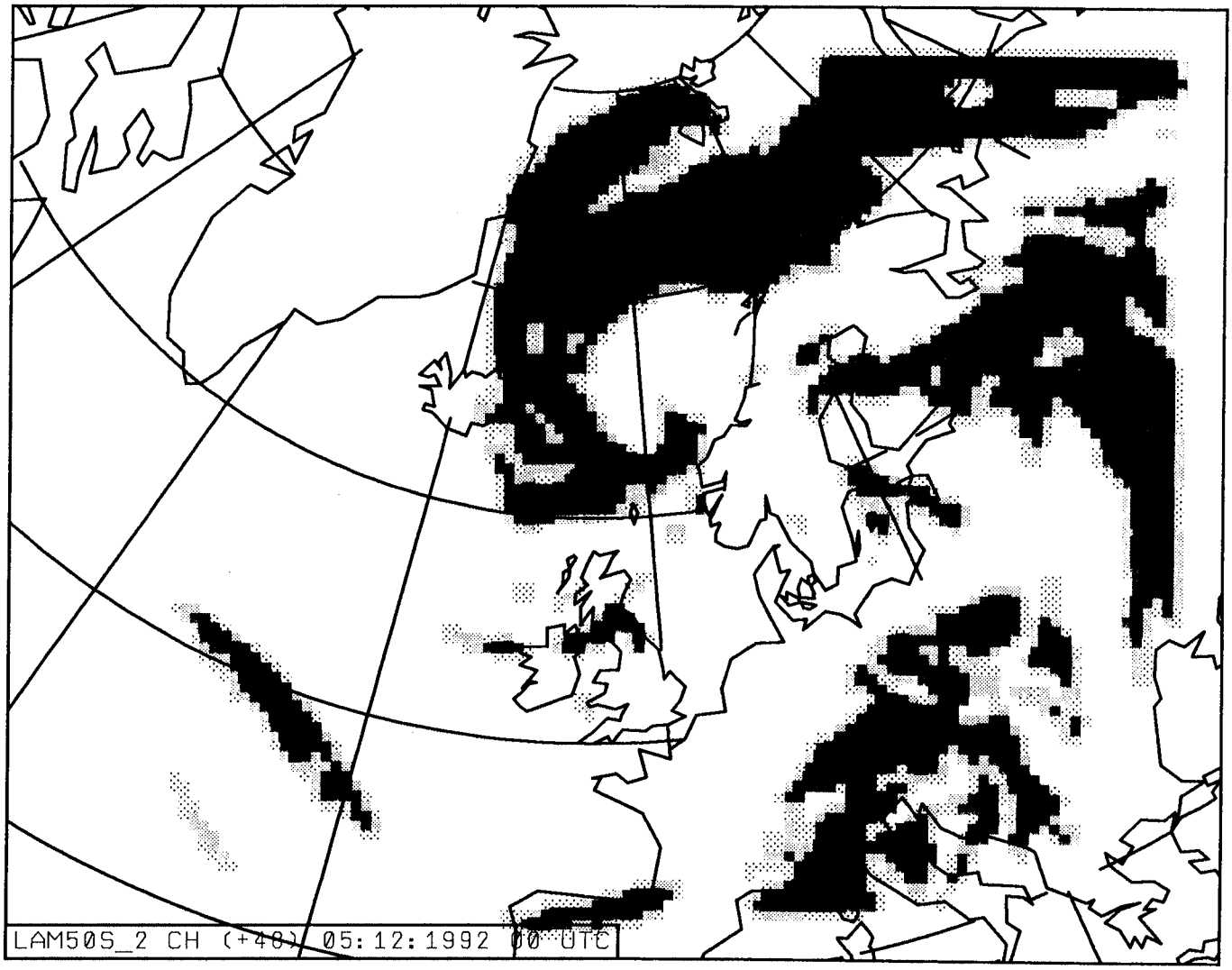


Figure 9d: As Fig. 9a, but for high clouds using nor-50.

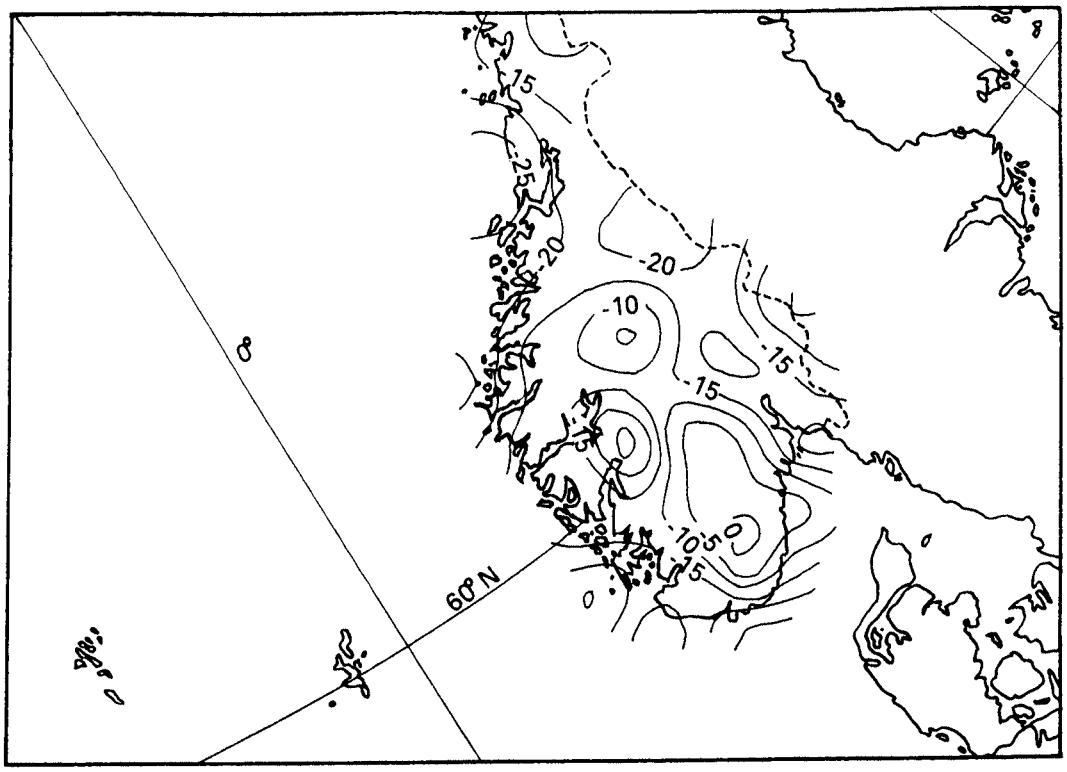


Figure 10a: The average differences between forecasted and observed cloudiness for sund-50 in November. The differences were interpolated from the irregular observation grid to a regular grid by use of simple kriging.

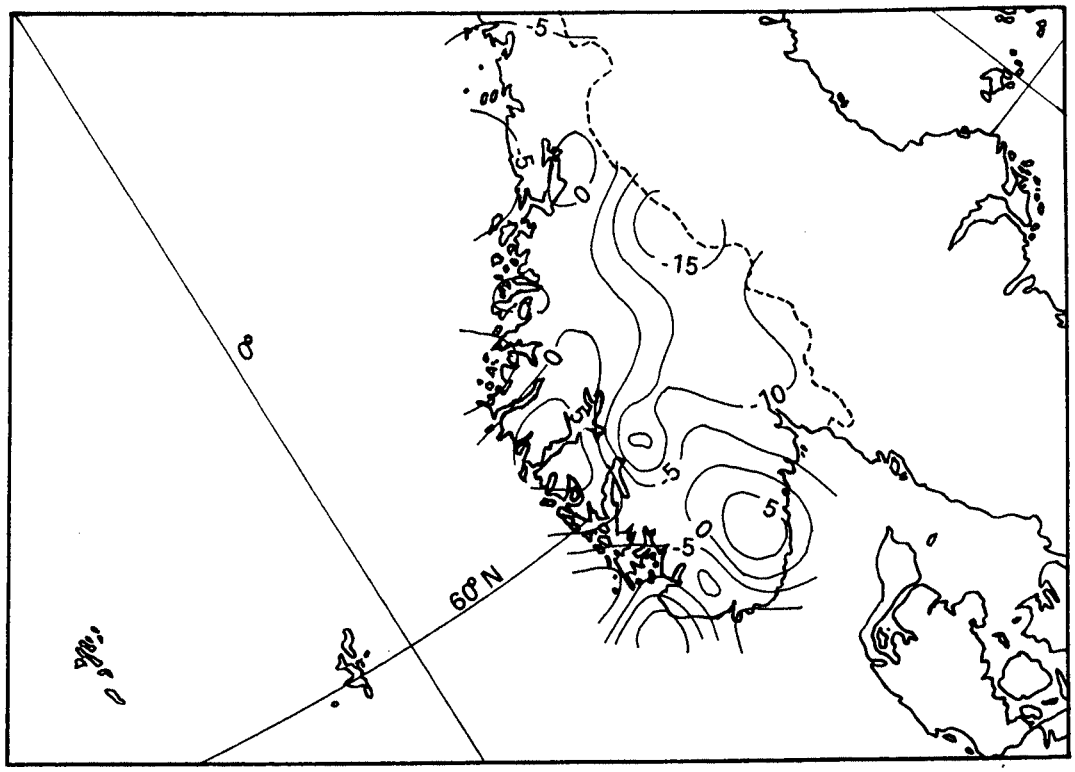


Figure 10b: As Figure 10a, but for nor-50.

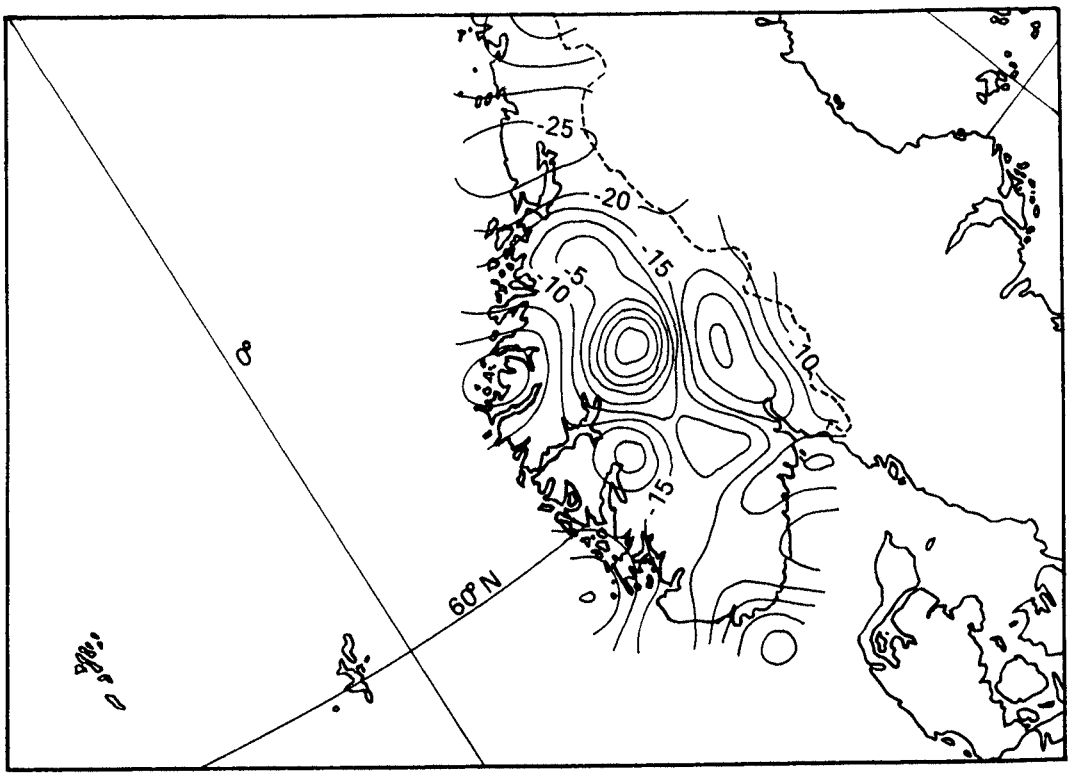


Figure 10c: As Figure 10a, but for sund-50 in December.

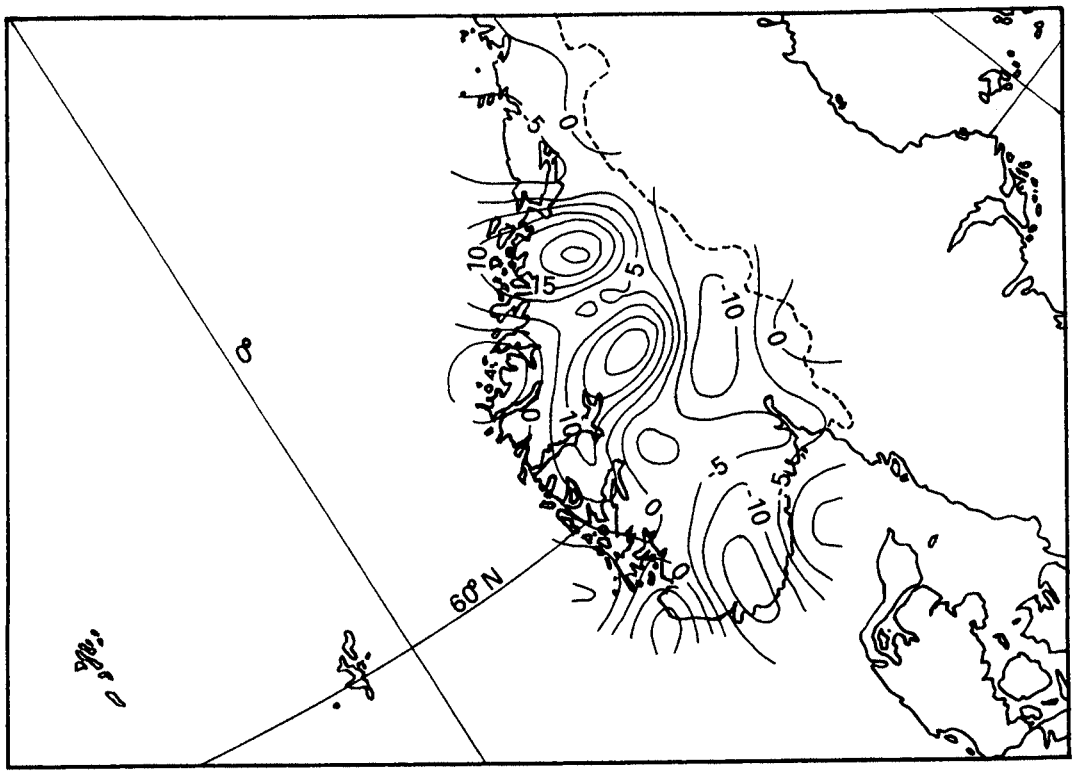


Figure 10d: As Figure 10a, but for nor-50 in December.

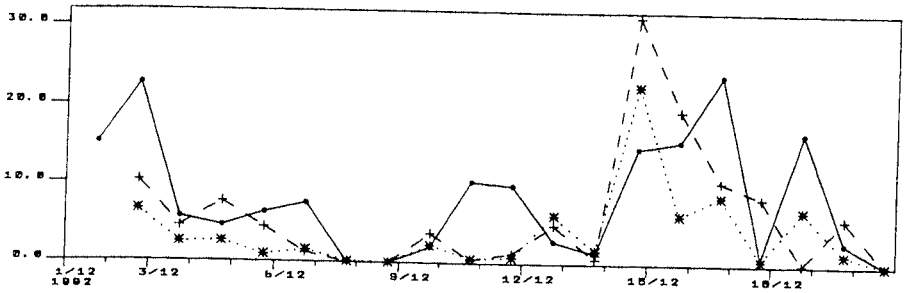


observation 12 UTC
nor-50 00 + 36 hours
sund-50 00 + 36 hours

| | STDE | RMSE | BIAS | CORR | N |
|---|---|---|---|---|---|
| nor-50 | 7.7 | 7.9 | -1.7 | 0.48 | 19 |
| sund-50 | 6.1 | 7.3 | -4.0 | 0.58 | 19 |

Figure 11: As Figure 3, but for 12 hour accumulated precipitation.

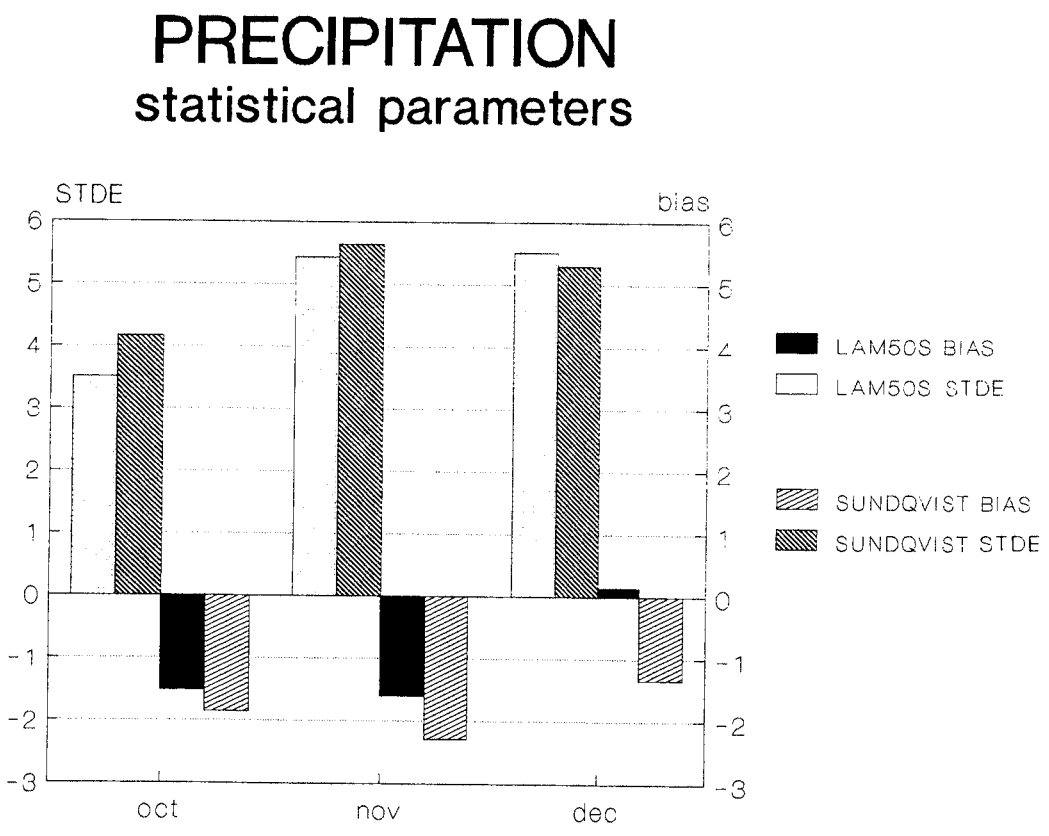


Figure 12: Standard deviation of errors, STDE, and bias for 36 hour model forecasts of 12 hour accumulated precipitation. The results include all the observing stations and are given for the three periods October, November and December.

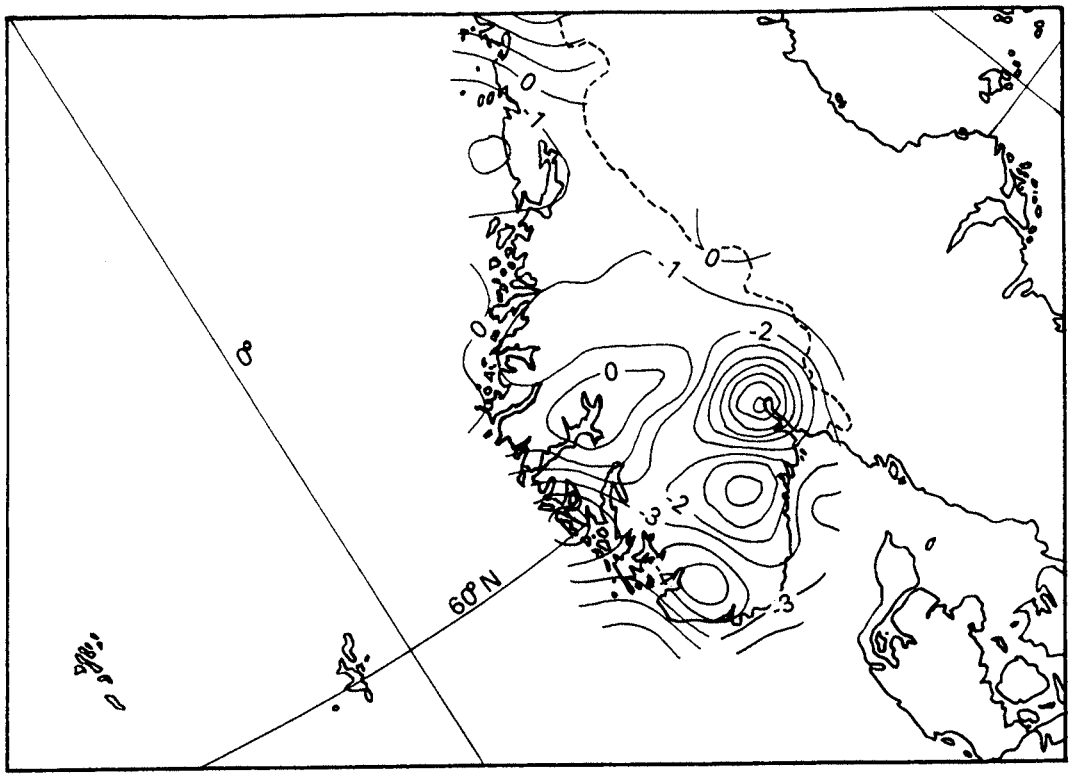


Figure 13a: The average differences between forecasted and observed precipitation for sund-50 in November. The differences were interpolated from the irregular observation grid to a regular grid by use of simple kriging.

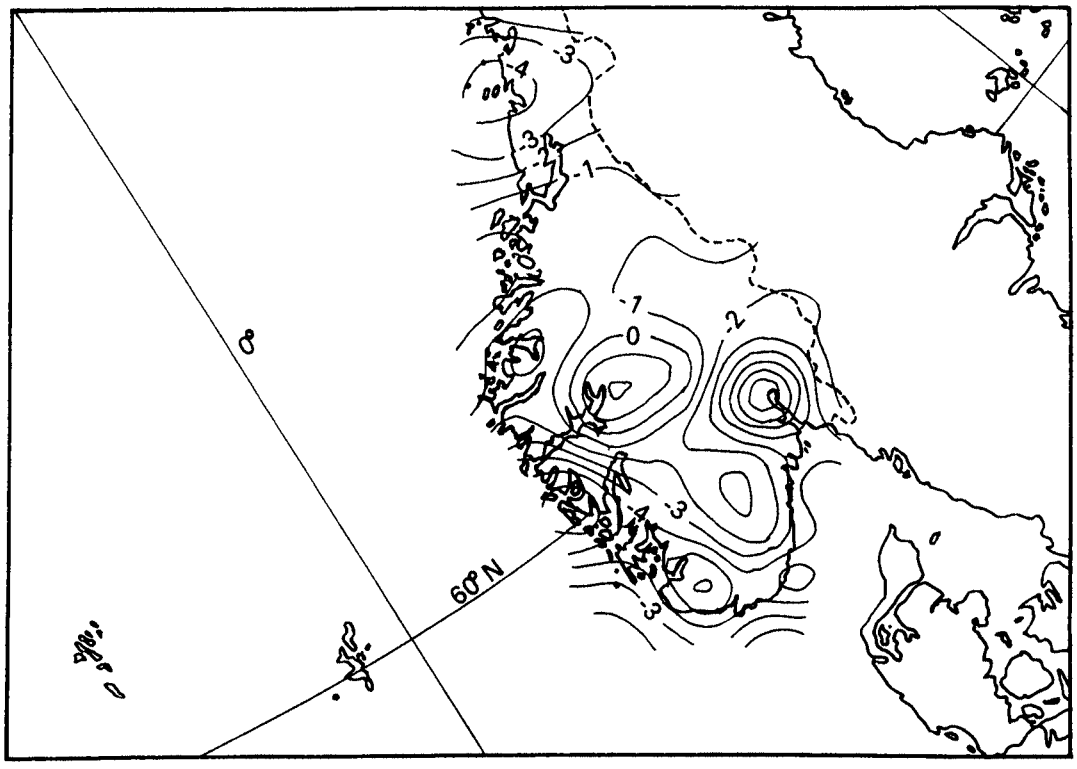


Figure 13b: As Figure 13a, but for nor-50.

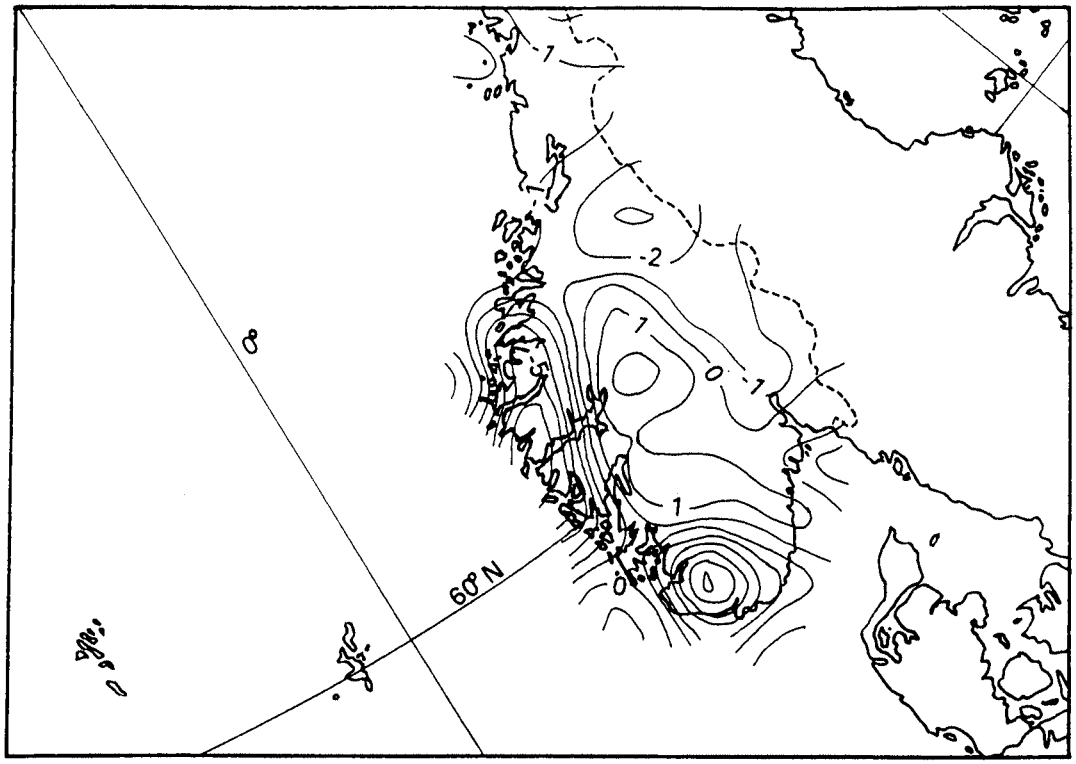


Figure 13c: As Figure 13a, but for sund-50 in December.

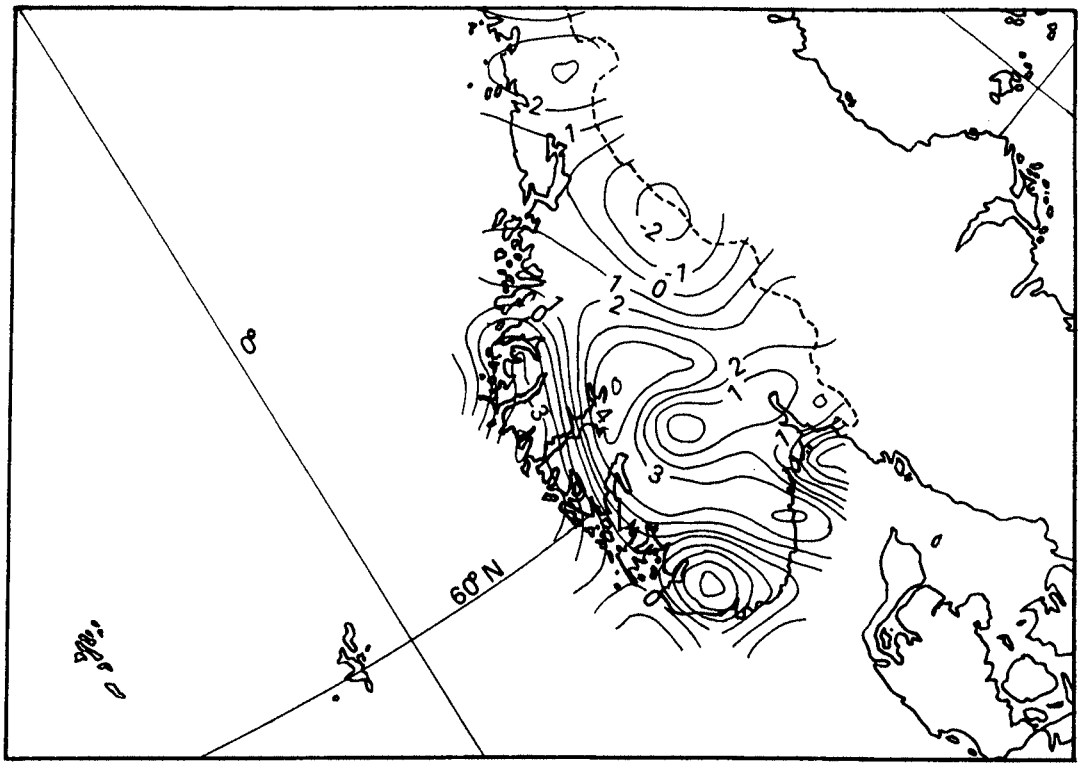


Figure 13d: As Figure 13a, but for nor-50 in December.